

# Voxel-Wise Logistic Regression for White Matter Hyperintensity Segmentation in FLAIR MRI

Jesse Knight <sup>a</sup>, Graham Taylor <sup>a</sup>, April Khademi <sup>b</sup>  
<sup>a</sup> University of Guelph, <sup>b</sup> Ryerson University

## 1 Introduction

White matter hyperintensities (WMH) are regions of increased signal intensity in T2-weighted brain MRI which are attributable to inflammation or erosion of tissue structure [1]. WMH are correlated with several neurodegenerative diseases, including cerebrovascular diseases, and certain types of dementia [2]. Automation of WMH segmentation is an active area of research, since it promises to facilitate large-scale studies with higher throughput and reduced human error [3]. Several segmentation competitions have sought to compare the recently proposed methods under standardized conditions [4, 5], including the 2017 WMH competition, to which this work relates. We briefly describe our submitted method to this competition here.

## 2 Method

The objective of the segmentation model is to predict the probability of the WMH class for each location, or voxel, in the input image. We assume the conditional probability of the lesion class  $c = 1$ , in one location  $x$ , given the features  $\mathbf{y} = [1, y^1, \dots, y^k]^T$ , can be modelled with a logistic function, parameterized by feature weights  $\boldsymbol{\beta} = [\beta^0, \beta^1, \dots, \beta^k]^T$ . Specifically, we have

$$\hat{c} = P(c = 1 | \mathbf{y}, \boldsymbol{\beta}) = \frac{1}{1 + e^{-\boldsymbol{\beta}^T \mathbf{y}}} \quad (1)$$

In a classic regression model, the parameters  $\boldsymbol{\beta}$  are fixed for all locations. However, we consider subjects in a standardized space (e.g. MNI) in which each voxel may have unique parameters – i.e. voxel-wise logistic regression (VLR). This overcomes problems of class separability by graylevel alone, while avoiding the use of unconditional spatial priors. Using a set of training data in a standardized space, the parameters are fitted *independently* for every voxel, yielding one set of parameters per voxel, or, equivalently, one image per parameter. In order to prevent overfitting, the model is estimated using MAP with a Gaussian prior on  $\boldsymbol{\beta}$  ( $L_2$  Regularization). For computational reasons, the log-likelihood of the model given the training data is maximized, as in

$$\boldsymbol{\beta}^* = \arg \max_{\boldsymbol{\beta}} \log L(\boldsymbol{\beta}) - \lambda \|\boldsymbol{\beta}\|_2 \quad (2)$$

$$= \arg \max_{\boldsymbol{\beta}} \sum_{n=1}^N [c_n \boldsymbol{\beta}^T \mathbf{y}_n - \log(1 + e^{\boldsymbol{\beta}^T \mathbf{y}_n})] - \lambda \|\boldsymbol{\beta}\|_2 \quad (3)$$

At test time, the estimated parameter images can be warped to the subject space, and used for inference, as in (1).

### 2.1 Implementation

While the VLR model is flexible to any set of feature images  $\mathbf{Y}(x)$ , we use only the FLAIR image. Warping of training and test images to MNI space is achieved using the Segment tool in SPM12 [6]. This also produces bias-corrected images, which are used thereafter in place of the originals. Since graylevel features from different MRI sources require standardization before they can be used in either training or testing contexts, we match the histogram of each volume to a target histogram:  $p(y) = \mathcal{N}(\mu = 0.5, \sigma = 0.12)$ . Following initial prediction by the VLR model, probabilistic output lesion masks are thresholded at a value which maximizes the mean training Similarity Index (AKA F1 score). Lesions less than 5 mm<sup>3</sup> are removed. The proposed algorithm is summarized in Figure 1. The training data used to estimate  $\boldsymbol{\beta}(x)$  are from previous competitions, summarized in Table 1. These data are augmented using sagittal mirroring and shifting by one voxel in all directions.

Table 1: Summary of augmented training image database.

Img (#)	Dataset	Ref.	Scanners	Manuals (#)
20+20+20	WMH SEG 2017	—	3T Philips Achieva, 3T Siemens TrioTim, 3T GE Signa HDxt	1 <sup>a</sup>
5+5+5	MS SEG 2016	[5]	3T Philips Ingenia, 1.5T Siemens Aera, 3T Siemens Verio	7 <sup>b</sup>
21	MS ISBI 2015	[4]	3T Philips	2 <sup>c</sup>

<sup>a</sup> Used only WMH labels; <sup>b</sup> Manuals fused using LOP-STAPLE; <sup>c</sup> Manuals fused using logical ‘and’.

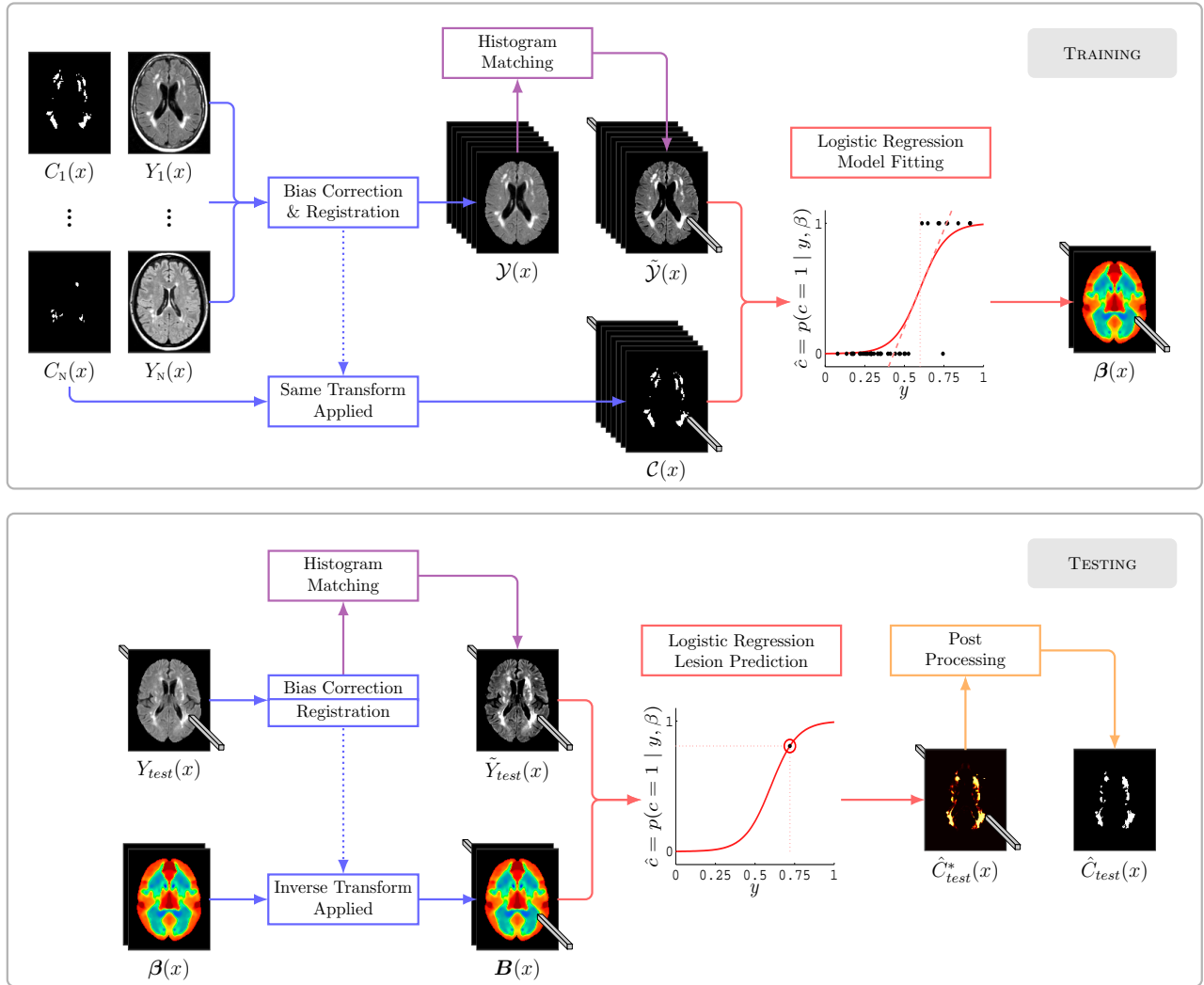


Figure 1: Overview of Voxel-wise Logistic Regression (VLR) algorithm. Roman typeface denote images in subject space, while calligraphic typeface denote images in standard space; image sets are bold;  $C(x)$ : manual segmentation;  $Y(x)$ : FLAIR image,  $\beta(x)$ : parameter image;  $\hat{C}(x)$ : estimated lesion segmentation.

## References

- [1] Joanna M Wardlaw, Maria C Valdés Hernández, and Susana Muñoz-Maniega. “What are white matter hyperintensities made of? Relevance to vascular cognitive impairment.” In: *Journal of the American Heart Association* 4.6 (June 2015), p. 001140. DOI: [10.1161/JAHA.114.001140](https://doi.org/10.1161/JAHA.114.001140).
- [2] S. Debette and H. S. Markus. “The clinical importance of white matter hyperintensities on brain magnetic resonance imaging: systematic review and meta-analysis”. In: *BMJ* 341 (July 2010). DOI: [10.1136/bmj.c3666](https://doi.org/10.1136/bmj.c3666).
- [3] Daniel Garcia-Lorenzo et al. “Review of automatic segmentation methods of multiple sclerosis white matter lesions on conventional magnetic resonance imaging.” eng. In: *Medical image analysis* 17.1 (Jan. 2013), pp. 1–18. DOI: [10.1016/j.media.2012.09.004](https://doi.org/10.1016/j.media.2012.09.004).
- [4] Aaron Carass et al. “Longitudinal multiple sclerosis lesion segmentation data resource”. In: *Data in Brief* 12 (June 2017), pp. 346–350. DOI: [10.1016/j.dib.2017.04.004](https://doi.org/10.1016/j.dib.2017.04.004). URL: [iacl.ece.jhu.edu/index.php/MSChallenge](http://iacl.ece.jhu.edu/index.php/MSChallenge).
- [5] *MS Lesion Segmentation Challenge 2016*. 2016. URL: <https://portal.fli-iam.irisa.fr/msseg-challenge>.
- [6] John Ashburner and Karl J Friston. “Unified segmentation.” eng. In: *NeuroImage* 26.3 (July 2005), pp. 839–851. DOI: [10.1016/j.neuroimage.2005.02.018](https://doi.org/10.1016/j.neuroimage.2005.02.018).

## Acknowledgements

The research was supported in part by the Natural Science and Engineering Research Council of Canada (NSERC-CGS-M) and by the Ontario Ministry of Advanced Education and Skills Development (OGS-M).